https://doi.org/10.5194/egusphere-2024-3250
Preprint. Discussion started: 10 December 2024

Modeling memory in gravel-bed rivers: A flow history-dependent relation for evolving thresholds of motion

Claire C. Masteller[1], Joel P.L. Johnson[2], Dieter Rickenmann[3], and Jens M. Turowski[4]

[1]Department of Earth, Environmental, and Planetary Sciences, Washington University in St. Louis, USA
[2]Jackson School of Geosciences, University of Texas at Austin, USA
[3]WSL Swiss Federal Institute for Forest, Snow, and Landscape Research, Switzerland
[4]Helmholtz Centre Potsdam, GFZ German Research Centre for Geosciences, Germany

Correspondence to: Claire C. Masteller (cmasteller@wustl.edu)

Abstract. Thresholds of motion (τ_c^*) strongly control bedload transport in gravel-bed rivers. Uncertainty in τ_c^* limits the accuracy of predictions of transport and morphologic change. To improve our quantitative understanding of morphodynamic feedbacks in rivers, we propose a flow history-dependent model where τ_c^* evolves temporally as a function of bed shear stress. Relatively low shear stresses strengthen the bed, increasing τ_c^* and reducing transport. Larger floods rapidly weaken the bed, decreasing τ_c^* and increasing transport. We calibrate the model to a 23-year record of flow and bedload transport from the Erlenbach Torrent, Switzerland, and find that the model predicts the field-based τ_c^* record more accurately than assuming a constant τ_c^*. Calibrated parameters describing strengthening are more tightly distributed than weakening parameters, which suggests that flood-induced bed weakening is more stochastic and less predictable than strengthening.

1 Introduction

Erosion, deposition and morphological change in gravel-bed rivers implies bedload transport. Models for bedload transport often include a threshold parameter, typically interpreted to represent the onset of sediment motion (e.g., Engelund & Fredsoe, 1976; Luque & Beek, 1976; Meyer-Peter & Müller, 1948; Wong & Parker, 2006; Shields, 1936; Wiberg & Smith, 1987). Transport often occurs close to threshold conditions even during floods, making transport rate predictions particularly sensitive to threshold values (e.g. Parker, 1978; Phillips & Jerolmack, 2016; Phillips et al., 2022; Pretzlav et al., 2020). Erosion thresholds also modulate the mapping of climate onto fluvial processes, informing short- and long-term sediment fluxes and the relative importance of extreme events for channel evolution (e.g. Blom et al., 2017; DiBiase & Whipple, 2011; Lague et al., 2005; Shobe et al., 2018; Tucker & Bras, 2000).

Early work assumed that, when nondimensionalized accounting for fluid density and grain weight per unit area, termed critical Shields stress, τ_c^*, that this threshold parameter should attain an essentially constant value for typical conditions in gravel-bed rivers (e.g. Buffington & Montgomery, 1997; Shields, 1936). However, Buffington & Montgomery (1997)

https://doi.org/10.5194/egusphere-2024-3250
Preprint. Discussion started: 10 December 2024

showed that τ_c^* varied systematically with the ratio of D_{50} (median grain size) to flow depth, and argued that a universal threshold should be applied with caution. More recent work has explored how both flow and grain interactions lead to inherent variability in τ_c^*. τ_c^* is observed to vary spatially with channel morphology and can be influenced by variations in slope (Lamb et al., 2008; Mueller et al., 2005), reach-scale bed morphology (Monsalve & Yager, 2017; Powell & Ashworth, 1995; Roberts et al., 2020), and changes in riverbed microtopography (Brayshaw, 1985; Hodge et al., 2019; Kirchner et al., 1990; Masteller & Finnegan, 2017; Yager et al., 2018).

Thresholds for motion can also evolve over time. For example, hysteresis in bedload transport rates is often observed between the rising and falling limbs of individual floods (Hsu et al., 2011; Mao, 2018; Mao et al., 2014; Pretzlav et al., 2020; Reid et al., 1985; Roth et al., 2017). Dynamic threshold evolution over the duration of a flood event is implied by the observed change in bedload transport rate. Changes in τ_c^* over multiple events have also been observed, and in most cases, τ_c^* values remain correlated across events, indicative of a memory of past conditions (Downs & Soar, 2021.; Hassan et al., 2020; Johnson, 2016; Lenzi et al., 2004; Mao, 2018; Masteller et al., 2019; Rickenmann, 2018, 2020; Saletti et al., 2015; Turowski et al., 2011).

Both variable flow strength and sediment supply can influence threshold evolution. Reid et al. (1985) first suggested the influence of antecedent flows based on field-based bedload transport monitoring, hypothesizing that longer inter-flood durations led to increases in τ_c^* and reduced sediment transport rates. Experiments have confirmed that the magnitude of inter-event flow affects τ_c^* evolution (Haynes & Pender, 2005; Masteller & Finnegan, 2017; Monteith & Pender, 2005; Ockelford et al., 2019; Ockelford & Haynes, 2013; Paphitis & Collins, 2005). With little to no active sediment transport, grain-scale changes in interlocking and surface reorganization increase particle resistance to motion (Masteller & Finnegan, 2017; Ockelford & Haynes, 2013; Yager et al., 2018). Pretzlav et al. (2020) documented systematic discharge-dependent increases and decreases in transport thresholds during several weeks of a snowmelt flood, using instrumented "smartrocks" to measure transport. Reduction of τ_c^* following larger floods has also been documented (Lenzi et al., 2004; Turowski et al., 2009; Yager et al., 2012), and has been attributed to significant reorganization of the riverbed. Increased sediment supply from channel banks and hillslopes can also be important in destabilizing the bed surface or introducing unconsolidated, more mobile material, reducing thresholds of motion (Turowski et al., 2011; Recking et al., 2012; Rickenmann, 2020). Building on observations by

https://doi.org/10.5194/egusphere-2024-3250
Preprint. Discussion started: 10 December 2024

Recking et al. (2012), Johnson (2016) developed a model in which τ_c^* evolves as a function of net erosion or deposition, which are controlled by sediment supply in relation to transport capacity. After calibration to laboratory experiments, the evolving-τ_c^* model successfully predicted how transport rates evolved during disequilibrium conditions caused by sediment pulses.

Using data from the Erlenbach torrent in Switzerland, Rickenmann (2020) calculated the degree of disequilibrium in bedload transport – interpreted to reflect variations in sediment supply – and showed that it correlated with evolving thresholds, supporting a supply dependence on thresholds. For the same stream, Masteller et al. (2019) showed that the magnitude of antecedent flows also influenced the evolution of τ_c^* for individual years. Consistent with experiments, Masteller et al. (2019) observed that the start of transport events showed increases in critical Shields stress with increasing inter-event flow magnitude (herein termed "strengthening") for an intermediate range of flows spanning inter-event periods and floods with observable sediment transport. However, following even higher-magnitude flows, the threshold for motion decreased (herein termed "weakening"). Masteller et al. (2019) hypothesized that the transition from bed strengthening to bed weakening was associated with a transition from local rearrangement of particles to more intense transport disrupting bed structure via particle collisions or long-distance particle transport, modified sediment supply through evacuation of bed sediments (Yager et al., 2012), or enhanced hillslope-channel coupling (Golly et al., 2017). Thus, both flow strength and sediment supply likely influence thresholds of motion in the Erlenbach torrent (Rickenmann, 2020; Masteller et al., 2019; Turowski et al., 2011), but the ability to predict the role of discharge-dependence remains elusive due to a lack of validated models.

While empirical evidence exists for systematic, flow strength-dependent temporal variations in thresholds for motion, few equations exist that quantify feedbacks leading to threshold evolution which can be incorporated into existing bedload transport models. Johnson's (2016) model predicts τ_c^* evolution as a function of sediment supply. Nonetheless, this model is an incomplete description of τ_c^* evolution because it does not account for riverbed strengthening or weakening directly caused by the flow. Our goals in the present work are (i) to propose a new model in which τ_c^* evolves as a function of flow magnitude and encapsulates some memory of past shear stresses as reflected in the changing state of the riverbed, and (ii) to evaluate whether the model can broadly capture annual strengthening and weakening trends as a function of discharge, as observed in Erlenbach field data (Masteller et al., 2019).

https://doi.org/10.5194/egusphere-2024-3250
Preprint. Discussion started: 10 December 2024

2 Model Development

Johnson (2016) argued that τ_c^* is a "state variable" for gravel-bed river morphodynamics because it simultaneously controls transport rates and evolves due to feedbacks with fluid shear stresses and transport rates. In our new model, changes in τ_c^* depend not only on discharge-dependent shear stress, but also on the current state of the transport system as characterized by τ_c^* itself. The rate of change of τ_c^* depends on two terms, which both evolve as a function of the transport capacity, τ^*/τ_c^*. Conceptually, the first term represents the contribution of any strengthening processes that may increase τ_c^*, while the second term represents any weakening processes that reduce τ_c^*:

$$\frac{\partial \tau_c^*}{\partial t} = k_1 B \left(1 + \left(\frac{\tau^*}{\tau_c^*}\right)^{-\gamma}\right)^{-1} - k_2 (1 - B) \left(\frac{\tau^*}{\tau_c^*} - 1\right)^{\varepsilon} H[\tau^*/\tau_c^* - 1], \quad (1)$$

where

$$B = \frac{\tau_{cmax}^* - \tau_c^*}{\tau_{cmin}^* - \tau_c^*}, \text{ with } \tau_{cmin}^* = 0.14S^{0.7} + 0.0075, \ \tau_{cmax}^* = 1.4S^{0.7} + 0.075. \quad (2)$$

Shields stress τ^* is equal to $\tau/(\rho_s\text{-}\rho)$gD, where τ, ρ_s, ρ, g and D are the dimensional bed shear stress, sediment density, water density, gravitational acceleration and median sediment diameter. t is time, and k_1 and k_2 are scaling factors on the strengthening and weakening terms of Equation 1, respectively. Exponents γ and ε influence the form and magnitude of the strengthening and weakening terms. H is the Heaviside step function ($H[\tau^*/\tau^*_c\text{-}1]$=0 for τ^*/τ^*_c<1; $H[\tau^*/\tau^*_c\text{-}1]$=1 for τ^*/τ^*_c>=1) such that weakening only occurs when transport is predicted. τ_{cmin}^* and τ_{cmax}^* are upper and lower bounds imposed on τ_c^*, and S is channel reach slope (an approximation of energy or water surface slope). τ_{cmin}^* and τ_{cmax}^* represent physical limits for how loosely-packed and mobile, or tightly-packed and immobile, the bed surface can become. Figure *S1* shows that the empirical τ_{cmin}^* and τ_{cmax}^* relations in Equation 2 capture the slope-dependence of gravel thresholds of motion compiled in both flume and field settings, while asymptoting to reasonable bounds at low channel slopes (e.g. Johnson, 2016; Lamb et al., 2008; Prancevic & Lamb, 2015). Our model is similar in form to that of Johnson (2016).

B is a "feedback parameter" because it contributes to $\partial\tau_c^*/\partial t$ being a function of τ_c^* (Johnson, 2016). B has a value between 0 and 1, and changes the relative importance of the strengthening and weakening terms, depending on the current

https://doi.org/10.5194/egusphere-2024-3250
Preprint. Discussion started: 10 December 2024

value of τ_c^* relative to τ_{cmin}^* and τ_{cmax}^* (Fig. 1). A loosely-packed bed, with τ_c^* close to τ_{cmin}^* and B close to 1, can strengthen significantly in a low flow (increasing τ_c^*), but a high flow would not cause a significant decrease in τ_c^*. Conversely, a bed that was already as tightly-packed as physically possible, with τ_c^* close to τ_{cmax}^* and B close to 0, cannot further increase τ_c^* in response to a low flow, but a destabilizing flood would cause a significant decrease in τ_c^* (Johnson, 2016).

Strengthening and weakening terms combine to cause increases and decreases in $\partial\tau_c^*/\partial t$ (Fig. 1). The strengthening term is generally sigmoidal for γ >1; it goes to zero as τ^* approaches zero, and asymptotes to a value of $k_1 B$ for $\tau^*/\tau_c^* \gg 1$ (Fig. 1a). Using a sigmoid allows strengthening over a wide range of flows, but limits how much strengthening can increase from changes in grain organization. When $\tau^*/\tau_c^* < 1$, flow causes the bed to become stronger but not weaker, consistent with previous observations (Haynes & Pender, 2005; Masteller et al., 2019; Masteller & Finnegan, 2017; Monteith & Pender, 2005; Ockelford et al., 2019). Strengthening increases as τ^*/τ_c^* approaches 1, consistent with some (Paphitis & Collins, 2005), but not all previous work (Haynes & Pender, 2007). Strengthening increases further for $\tau^*/\tau_c^* > 1$, consistent with protrusion-dependent thresholds (Masteller and Finnegan, 2017, Yager et al., 2018; Masteller et al., 2019), and with coarse grain clustering, which increases bed stability and requires transport to develop (Brayshaw, 1985; Church et al., 1998; Hassan et al., 2020; Johnson, 2017; Strom et al., 2004). At the same time, as τ^*/τ_c^* exceeds 1, the weakening term becomes increasingly important (Fig. 1). The combination of terms results in the transition from strengthening to weakening occurring at different τ^*/τ_c^*, depending on γ, ε, k_1, k_2, and τ_c^*. Higher shear stresses capable of mobilizing more sediment grains can destabilize a larger fraction of the bed. Impacts from transported grains may also directly contribute to destabilization (Ancey & Heyman, 2014; Heyman et al., 2014; Lee & Jerolmack, 2018; Martin et al., 2014). Nonetheless, we note that the model is agnostic towards any specific processes driving strengthening and weakening.

https://doi.org/10.5194/egusphere-2024-3250
Preprint. Discussion started: 10 December 2024

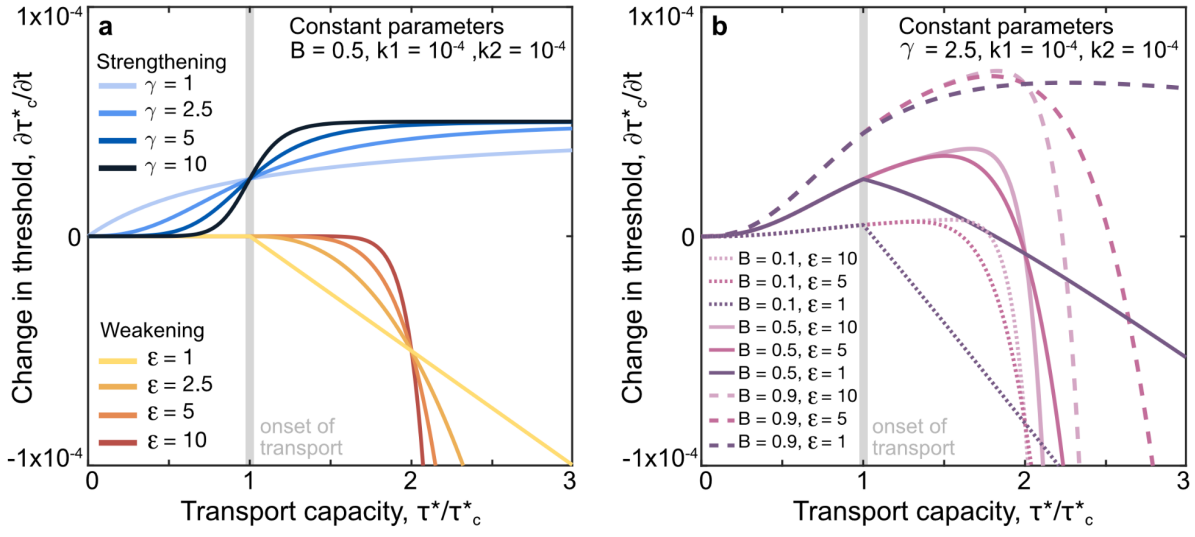

Figure 1: A) Predicted change in threshold for strengthening (blue) and weakening terms (red) for a range of γ and ε values. k_1, k_2, and B are constant. B) Predicted change in threshold for the full model with a specified B and ε. k_1, k_2, and γ are held constant. This example uses Erlenbach values $\tau^*_{cmin} = 0.036$, $\tau^*_{cmax} = 0.36$. Perceptually uniform scientific colourmaps were used (Crameri et al., 2020).

3 Field application

The Erlenbach is a small (0.7 km^2), steep (10% grade) channel in the Swiss Prealps. Bedload transport has been actively monitored for over 30 years by a variety of methods (Rickenmann & McArdell, 2007; Rickenmann, 2020). Previous analyses have shown that the threshold for motion varies significantly across the span of the record (Masteller et al., 2019; Turowski et al., 2011; Yager et al., 2012). Masteller et al. (2019) demonstrated that seasonal trends in τ^*_c were unlikely to be random; threshold evolution depends, in part, on the magnitude of past flows.

Our goal is to evaluate how well discharge-dependent shear stress variations alone (Equations 1 and 2) capture first-order seasonal trends in evolving τ^*_c from well-constrained field data. We utilize publicly available 23-year, 10-minute interval discharge and bedload transport records from the Erlenbach (Rickenmann et al., 2020). To calculate thresholds of motion for model comparison, we measure the discharge when the in-channel impact plate system registers grain collisions near the beginning of a flow event, following Turowski et al. (2011). Thus, the threshold data are independent of any bedload transport model. Using a rating curve from discharge to shear stress developed by Yager (2006) and a median grain size, D_{50} = 8 cm (Wyss et al. 2016), the flow and transport time series were nondimensionalized to Shields stress. The median grain size is

https://doi.org/10.5194/egusphere-2024-3250
Preprint. Discussion started: 10 December 2024

assumed to have not changed systematically across the Erlenbach record (as discussed by Masteller et al., 2019), although hillslope sediment supply may cause grain size variability both during and between transporting events.

Critical Shields stresses at the start of transport vary by almost an order of magnitude in τ_c^* (0.03 to 0.26). Strengthening (i.e., a systematic increase in τ_c^* for at least some portion of a given year) is dominant in 10 of the 23 years (see Masteller et al., 2019). Weakening is dominant in 3 years (1992, 2014, 2015), while the remaining 10 years exhibit some combination of these behaviors (Fig. 2e-h).

4 Model parameterization and application

We implement the model separately to each year's flow time series, from the first transporting event in the spring through the fall (following Masteller et al., 2019). We do not calibrate τ_c^* to the single continuous multi-year discharge and transport record because the bulk of landsliding occur during the winter months, supplying largely unconstrained amounts of sediment to the channel bed from hillslope processes (Schuerch et al., 2006). Hillslope sediment supply variations also occur during the rest of the year and likely influence thresholds and transport rates both during and in between the transporting events we consider (e.g., Rickenmann, 2020; 2024). As possible evidence of sediment supply effects during inter-event periods, Turowski et al. (2011) found that threshold discharges were often, though not always, lower at the start of a given flow event compared to the threshold discharge at the end of the previous event. This inter-event weakening cannot be captured by the model. Because the model cannot predict every trend in the field data, we focus on the start of events only in order to evaluate how well discharge variations alone can improve transport predictions over seasons, consistent with the analysis of Masteller et al. (2019). Future analyses could focus on threshold evaluation and model calibration during individual flood events.

Equation 1 has four free parameters: k_1, k_2, γ, and ε. We assign γ = 2.5±0.4 (at 95% confidence), which we independently calibrated using experiments by Paphitis and Collins (2005) over the range $\tau^*/\tau_c^* = 0.5$ to 0.9 (Supplementary Fig. *S2*). This leaves three parameters that require calibration. For each year, we explored a range of parameter combinations for k_1 (1×10^{-1} to 1×10^{-5}, n = 40), k_2 (1×10^{-1} to 1×10^{-5}, n = 10), and ε (1 to 10, n = 10). k_1 and k_2 were varied with log-spacing to explore all orders of magnitude equivalently. For each year of the dataset, we ran 16,000 forward simulations, reflecting all unique parameter combinations of k_1, k_2, and ε. For each year, we assign an initial τ_c^* value as equal to the observed τ_c^* at the

https://doi.org/10.5194/egusphere-2024-3250
Preprint. Discussion started: 10 December 2024

first transport event and calculate changes in τ_c^* based on 10-minute discharge data, until the end of the final observed transport event.

We determined the best-fit parameter combinations that minimized Mean Absolute Error (MAE) to τ_c^* data for each year. We use MAE (rather than RMSE) to reduce the influence of any single large difference between the continuous model predictions and outliers in rather noisy transport data, which only represent the discrete start of each event. "Annual" calibrations represent the best-fit parameters for each year. The "average" calibration represents the single best-fit k_1, k_2, and ε values which minimize MAE when MAE is averaged across all sample years, with each year weighted equally. We compare both the annual and average best-fit model to a constant τ_c^* (mean Erlenbach τ_c^* = 0.1547, SE = 0.0014).

5 Results

The annual calibrations show that, for all 23 years, Equation 1 provides a better fit to the data (lower MAE) than the mean Erlenbach threshold, τ_c^* = 0.1547 (Fig. 2a). Annual best-fit MAE ranges from 0.0046 (2015) to 0.0293 (1990). The median MAE = 0.0134 from the annual calibrations is less than the median MAE = 0.0219 when applying a constant τ_c^* = 0.1547. Annual best-fit values for k_1 ranged from 1×10^{-5} to 2.73×10^{-4} with a median value of 5.22×10^{-5} (Fig. 2b). In contrast, annual best-fit k_2 values spanned the entire parameter range (1×10^{-5} to 0.1) with median $k_2 = 4.12\times10^{-5}$ (Fig. 2c). Best-fit annual ε values also spanned the full range of parameter values explored (1 to 10) (Fig. 2c), with median ε = 6 when calculated with each year weighted equally.

https://doi.org/10.5194/egusphere-2024-3250
Preprint. Discussion started: 10 December 2024

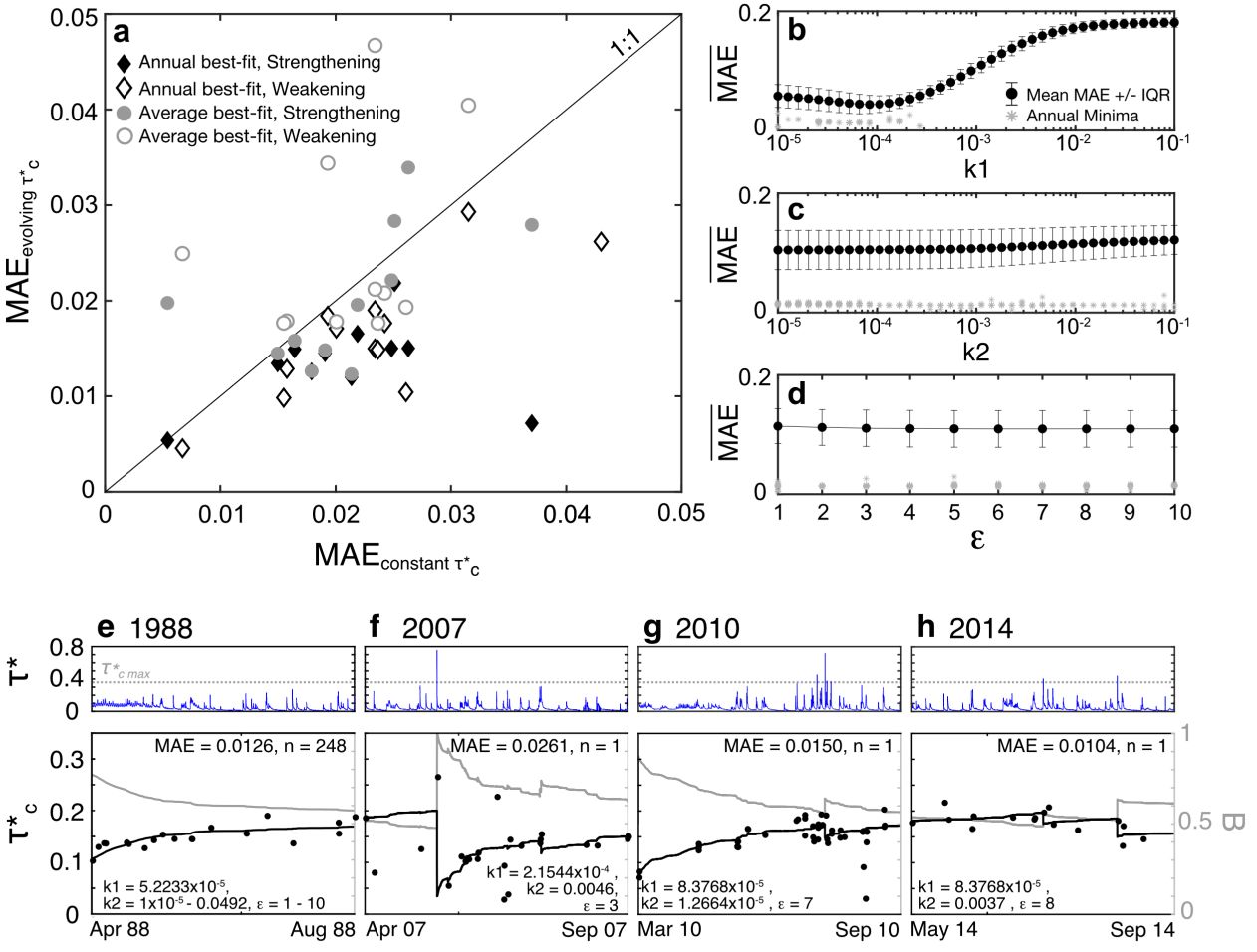

Figure 2: A) Comparison of MAE fits for constant and evolving τ^*_c values compared to τ^*_c data from the Erlenbach for both annually calibrated and average calibration models. (B-D) Mean and interquartile range of MAE for model runs binned by (B) k_1, (C) k_2, and (D) ε parameters. Annually minimum MAE and associated parameters indicated by grey stars. In the event of repeated minimum MAE (see discussion), all parameters resulting in a minimized MAE are plotted. (E-H) Example years with (E) strengthening only (1988), (F) dominantly weakening, with strengthening as well (2007), (G) dominantly strengthening, with weakening as well (2010), and (H) dominantly weakening (2014). Upper panels show the flow time series for each year in blue; model parameter $\tau^*_{cmax} = 0.36$ is also indicated. Feedback parameter B is shown for each year (right-hand y axis). "n" gives the number of models (i.e., parameter combinations) that minimize MAE and provide an equivalent best fit to the data. Annual best-fit parameters are also specified.

https://doi.org/10.5194/egusphere-2024-3250
Preprint. Discussion started: 10 December 2024

The single best-fit value from the "average" MAE analysis was also $\varepsilon = 6$, with average best-fit $k_1 = 5.22\times10^{-5}$ and $k_2 = 4.12\times10^{-5}$. These best-fit ε, k_1, and k_2 values are consistent when averaging MAE across all years and when only averaging for the eight years with predicted weakening behavior (step drops in $\tau_c^* > 2\%$). Model runs using these average best-fit parameters only perform better than the constant τ_c^* assumption in 12 out of 23 sample years (median MAE = 0.217) (Fig. 2a). Both annual and average model performance is generally better for years which only have τ_c^* strengthening, as evidenced by annual median MAE = 0.0145 (average median MAE = 0.0198) for these years compared to years with observed weakening (annual median MAE = 0.018; average median MAE = 0.0282). In 11 years, multiple combinations of parameters can give the same minimum MAE value. Most of these years only have systematic strengthening, not weakening, so models are relatively insensitive to k_2 and ε values, allowing a range of best-fit model parameters. The field data tend to be more variable in years with weakening; nonetheless the calibrated model captures first-order, annual trends across a range of scenarios (Fig. 2e-h, Fig. S3). Across all examples, the dominance of the strengthening effects is demonstrated by B>0.5.

Comparison of mean MAE values of all model runs as a function k_1, k_2, and ε elucidates the relative sensitivity of model performance to each parameter (Fig 2 b-d). Model performance was most sensitive to k_1 for the parameter space we explored, with mean MAE values ranging from MAE = 0.0441 at $k_1 = 8.38\times10^{-5}$ to MAE = 0.185 at $k_1 = 0.1$, reflecting the clustering of best-fit k_1 values (Fig. 2b). We note that $\gamma = 2.5$ was independently calibrated; it is possible that if our analysis also explored a range of γ values, then the range of acceptable k_1 may be broader. In contrast, mean MAE values are higher and less variable when binned by k_2 (MAE = 0.108-0.124) and ε (MAE = 0.113-0.117), suggesting that annual model performance is less sensitive to variations in these parameters (Fig. 2b,c).

6 Discussion and Conclusion

Our flow-history model for τ_c^* (Equations 1, 2) performs better than a constant entrainment threshold, as indicated by lower MAE between data and model (Fig. 2a). The model captures both first-order strengthening and weakening trends seen in the field data. These include progressive increases in τ_c^* from lower discharges (Fig. 2e), to sudden decreases in τ_c^* following a large flood early in the season (Fig. 2f), to a smaller decrease in τ_c^* following a late-season flood after the riverbed may have had more time to strengthen (Fig. 2g), to intermittent but repeated weakening events across a season (Fig. 2h). When

https://doi.org/10.5194/egusphere-2024-3250
Preprint. Discussion started: 10 December 2024

each year is calibrated separately ("annual"), the model unsurprisingly performs better than when using the single set of parameters that minimizes MAE averaged across all years ("average"). Nonetheless, the "average" best-fit parameters still outperformed a constant τ_c^* assumption in a majority of years – particularly those with seasonal strengthening trends.

Calibrated model performance varies most with k_1, which governs the efficacy of strengthening (Fig. 2b, Eq. 1). γ also influences strengthening, but was independently calibrated and held constant in our analysis ($\gamma = 2.5$; Supplementary Fig. *S2*). At the Erlenbach, sediment-transporting flood events only comprise about 2% of the discharge record (Masteller et al., 2019). Weakening parameters k_2 and ε can only influence τ_c^* evolution during this portion of the record, when $\tau^*/\tau_c^* > 1$ (Equation 1). High values of ε and B result in τ_c^* weakening only becoming dominant at even higher transport capacities (Fig. 1). In years without large floods, the strengthening term of Equation 1 dominates for the majority of the year, resulting in steady increases in τ_c^*, such as in 1988 when floods did not exceed $\tau^*/\tau_c^* = 1.64$ (Fig. 2e). Therefore, 1988 best-fit models were insensitive to k_2 and ε, resulting in 248 parameter combinations that minimized MAE (Fig. 2e). More broadly, because gravel-bed river geometry has been suggested to adjust so that bankfull flows only just exceed the threshold for motion (Parker 1978, Phillips and Jerolmack, 2016), weakening processes, which in our model only occur when $\tau^*/\tau_c^* \geq 1$, can only reduce τ_c^* for a limited fraction of the full discharge record. Thus, we may expect more generally that strengthening processes are dominant for the majority of the time in gravel river beds relative to weakening processes that may only occur during floods. The consequences of this difference in the total time over which strengthening and weakening processes may occur and their resultant impact on the time-averaged state of the riverbed, as reflected by τ_c^*, is not explored here, but should explored in future work. At the Erlenbach, the success of the model in matching annual strengthening trends (Fig. 2a, e-h) with a narrow distribution of best-fit k_1 values and a single, independently-calibrated value of $\gamma = 2.5$ suggests that the physical processes that are encapsulated in the strengthening term of Equation 1 may be more consistent and predictable across the full discharge record in similar field settings and that they may be further interrogated by flume experiments (e.g. Church et al., 1998; Masteller & Finnegan, 2017; Ockelford & Haynes, 2013).

In contrast, calibrations of weakening parameters find much more variability in best-fit ε and k_2, and MAE is higher for weakening years (Fig. 2a). Annual best-fit results span the full range of both parameters (Fig. 2c,d). High-magnitude floods, one mechanism that can cause weakening, are relatively rare and short-lived; it is possible that a data set with many more

https://doi.org/10.5194/egusphere-2024-3250
Preprint. Discussion started: 10 December 2024

discharge-driven weakening events could more narrowly constrain these variables. However, a simpler interpretation consistent with our analysis is that weakening is inherently more stochastic and difficult to predict. Weakening events can be de-coupled from flow, for example, if hillslopes supply sediment to the channel during inter-event periods, leading to a reduction in τ_c^* at low discharge. Indeed, Masteller et al. (2019) identified a minimum discharge for inter-event strengthening, below which τ_c^* becomes uncorrelated with flow magntiude. This loss of correlation likely indicates instances where supply effects introduce event-scale variability in τ_c^*. While this paper focuses on evaluating a discharge-driven model for τ_c^* , it is not intended to fully address all factors influencing variability in τ_c^*. The discrepancies between observed τ_c^* and model predictions may highlight conditions where sediment supply significantly alters bed mobility, outweighing the flow history effects that are addressed here.

Fig. 2e-h illustrates how feedback parameter B controls how τ_c^* changes in response to a given shear stress. Low τ_c^* (such as at the start of the 1988 and 2010, and following the large 2007 flood) corresponds to high B, which increases the strengthening term and reduces the weakening term (Equations 1,2). As relatively smaller shear stresses lead to progressive strengthening, τ_c^* increases, B decreases, and less strengthening occurs for a given increment of shear stress, resulting in a gradual rollover in the rate of strengthening through time (e.g., Fig. 2e). Model response (i.e., $\partial\tau_c^*/\partial t$) is also influenced by τ_c^* through changes in transport capacity. For example, under strengthening conditions, even if τ^* remains constant, increasing τ_c^* would cause a gradual decrease in τ^*/τ_c^*, slowing the rate of strengthening.

Thus, the "memory" in this model is represented by the value of τ_c^*, which integrates the effects of the past history of both flow conditions and channel bed conditions. Model memories tend to be asymmetric through time in that floods large enough to cause significant weakening will rapidly reset the memory to lower τ_c^* values; strengthening can only occur gradually as it requires the cumulative effects of lower discharges over time. Conceptually, these memory effects relate to τ_c^* being a state variable for gravel-bed channels (Johnson, 2016); by knowing τ_c^*, one can predict future channel response to floods. We view this model as a step towards a more complete understanding of mountain river morphodynamics. Our calibrated τ_c^* equation should be useful for improved modeling of channel transport and evolution, and as a component of landscape evolution modeling. When high-resolution discharge data is available for field sites, incorporation of a flow-

https://doi.org/10.5194/egusphere-2024-3250
Preprint. Discussion started: 10 December 2024

dependent τ_c^* may improve quantitative predictions of transport in gravel-bed rivers, although calibration to local conditions is likely necessary.

Perhaps the biggest mechanistic limitation of our model is that it only accounts for discharge controls on evolving thresholds, even though sediment supply and transport disequilibrium have been shown to explicitly influence transport rates in the Erlenbach data (Rickenmann, 2020; 2024). Future work could attempt to disentangle how sediment supply influences our parameter calibrations. These best-fit model parameter values found in this study could be used as specific predictions to be independently tested using other field and flume data. Model performance could also be assessed at the scale of individual events using continuous bedload measurements, rather than just thresholds at the start of events as done here. The model does not try to isolate granular interaction-based processes that likely cause strengthening and weakening, but rather lumps processes together using empirical parameters. Quantifying the systematics, inherent variability, and dominant processes involved in bed weakening warrants additional study. We suggest that a combination of discharge-based controls on τ_c^* (as explored here) and sediment-supply controls on τ_c^* (e.g., Recking, 2012; Johnson, 2016; Rickenmann, 2020; Rickenmann, 2024) may be able to explain much of the deterministic variability in threshold evolution and sediment transport rates in gravel-bed rivers.

Code availability

A working version of the code used to complete the model runs, associated best-fit model runs, and a summary of MAE values for all model runs produced during this research are publicly available through Zenodo (Masteller et al., 2024). Due to file upload limits of Zenodo, additional model runs are available by request to the corresponding author.

Note to the Editor and Reviewers – All data will be made publicly availably on Zenodo, however, the data are not yet formally published with a DOI. The formally published data will be cited here and linked with a DOI following review. This delay is to enable edits to the dataset if substantive methodological changes are suggested during the review process resulting in material changes to the data.

https://doi.org/10.5194/egusphere-2024-3250
Preprint. Discussion started: 10 December 2024

Data availability

The discharge and sediment transport time series data from the Erlenbach is publicly available at Rickenmann et al. (2020).

Author contribution

J. Johnson and C. Masteller formulated the concept of the study and the state function. C. Masteller completed the model runs, calibration, and error analysis. Field data were collected and provided by D. Rickenmann and J.M. Turowski. The manuscript was written by C. Masteller with contributions from all authors.

Competing interests

Some authors are members of the editorial board of journal Earth Surface Dynamics.

References

Ancey, C. and Heyman, J.: A microstructural approach to bed load transport: mean behaviour and fluctuations of particle transport rates, Journal of Fluid Mechanics, 744, 129–168, https://doi.org/10.1017/jfm.2014.74, 2014.

Blom, A., Arkesteijn, L., Chavarrías, V., and Viparelli, E.: The equilibrium alluvial river under variable flow and its channel-forming discharge, Journal of Geophysical Research: Earth Surface, 122, 1924–1948, https://doi.org/10.1002/2017JF004213, 2017.

Brayshaw, A. C.: Bed microtopography and entrainment thresholds in gravel-bed rivers, GSA Bulletin, 96, 1985.

Buffington, J. M. and Montgomery, D. R.: A systematic analysis of eight decades of incipient motion studies, with special reference to gravel-bedded rivers, Water Resources Research, 33, 1993–2029, https://doi.org/10.1029/96WR03190, 1997.

Chen, L. and Stone, M. C.: Influence of bed material size heterogeneity on bedload transport uncertainty, Water Resources Research, 44, 2008.

Church, M., Hassan, M. A., and Wolcott, J. F.: Stabilizing self-organized structures in gravel-bed stream channels: Field and experimental observations, Water Resources Research, 34, 1998.

Crameri, F., Shephard, G. E., and Heron, P. J.: The misuse of colour in science communication, Nat Commun, 11, 5444, https://doi.org/10.1038/s41467-020-19160-7, 2020.

https://doi.org/10.5194/egusphere-2024-3250
Preprint. Discussion started: 10 December 2024

DiBiase, R. A. and Whipple, K. X.: The influence of erosion thresholds and runoff variability on the relationships among topography, climate, and erosion rate, J. Geophys. Res., 116, F04036, https://doi.org/10.1029/2011JF002095, 2011.

Dietrich, W. E., Kirchner, J. W., Ikeda, H., and Iseya, F.: Sediment supply and the development of the coarse surface layer in gravel-bedded rivers, Nature, 340, 215–217, https://doi.org/10.1038/340215a0, 1989.

Downs, P. W. and Soar, P. J.: Beyond Stationarity: Influence of Flow History and Sediment Supply on Coarse Bedload Transport, Water Resources Research, n/a, e2020WR027774, https://doi.org/10.1029/2020WR027774, n.d.

Engelund, F. and Fredsoe, J.: A Sediment Transport Model for Straight Alluvial Channels, Nord Hydrol, 7, https://doi.org/10.2166/nh.1976.0019, 1976.

Golly, A., Turowski, J. M., Badoux, A., and Hovius, N.: Controls and feedbacks in the coupling of mountain channels and hillslopes, Geology, 45, 307–310, https://doi.org/10.1130/G38831.1, 2017.

Gran, K. B., Montgomery, D. R., and Sutherland, D. G.: Channel bed evolution and sediment transport under declining sand inputs, Water Resources Research, 42, https://doi.org/10.1029/2005WR004306, 2006.

Hassan, M. A., Saletti, M., Johnson, J. P. L., Ferrer-Boix, C., Venditti, J. G., and Church, M.: Experimental Insights Into the Threshold of Motion in Alluvial Channels: Sediment Supply and Streambed State, Journal of Geophysical Research: Earth Surface, 125, e2020JF005736, https://doi.org/10.1029/2020JF005736, 2020.

Haynes, H. and Pender, G.: Flume investigation into the influence of shear stress history, Water Resources Research – Water Resources Research, 41, 2005.

Haynes, H. and Pender, G.: Stress History Effects on Graded Bed Stability, Journal of Hydraulic Engineering, 133, 2007.

Heyman, J., Ma, H. B., Mettra, F., and Ancey, C.: Spatial correlations in bed load transport: Evidence, importance, and modeling, Journal of Geophysical Research: Earth Surface, 119, 1751–1767, https://doi.org/10.1002/2013JF003003, 2014.

Hodge, R. A., Sear, D. A., and Leyland, J.: Spatial variations in surface sediment structure in riffle-pool sequences: a preliminary test of the Differential Sediment Entrainment Hypothesis (DSEH): Spatial Variations in Sediment Structure in Riffle-Pool Sequences, Earth Surf. Process. Landforms, 38, 449–465, https://doi.org/10.1002/esp.3290, 2013.

Hsu, L., Finnegan, N. J., and Brodsky, E. E.: A seismic signature of river bedload transport during storm events, Geophysical Research Letters, 38, https://doi.org/10.1029/2011GL047759, 2011.

Johnson, J. P. L.: Gravel threshold of motion: a state function of sediment transport disequilibrium?, Earth Surface Dynamics, 4, 685–703, https://doi.org/10.5194/esurf-4-685-2016, 2016.

Kirchner, J. W., Dietrich, W. E., Iseya, F., and Ikeda, H.: The variability of critical shear stress, friction angle, and grain protrusion in water-worked sediments, Sedimentology, 37, 647–672, https://doi.org/10.1111/j.1365-3091.1990.tb00627.x, 1990.

Lague, D., Hovius, N., and Davy, P.: Discharge, discharge variability, and the bedrock channel profile: DISCHARGE VARIABILITY AND CHANNEL PROFILE, J. Geophys. Res., 110, n/a-n/a, https://doi.org/10.1029/2004JF000259, 2005.

Mao, L., Dell'Agnese, A., Huincache, C., Penna, D., Engel, M., Niedrist, G., and Comiti, F.: Bedload hysteresis in a glacier-fed mountain river, Earth Surface Processes and Landforms, 39, 2014.

https://doi.org/10.5194/egusphere-2024-3250
Preprint. Discussion started: 10 December 2024

Martin, R. L., Purohit, P., and Jerolmack, D.: Sedimentary Bed Evolution as a Mean-Reverting Random Walk: Implications for Tracer Statistics, Geophysical Research Letters, 6152–6159, https://doi.org/10.1002/2014GL060525, 2014.

Masteller, C. C. and Finnegan, N. J.: Interplay between grain protrusion and sediment entrainment in an experimental flume, Journal of Geophysical Research: Earth Surface, 122, 2017.

Masteller, C. C., Finnegan, N. J., Turowski, J. M., Yager, E. M., and Rickenmann, D.: History-Dependent Threshold for Motion Revealed by Continuous Bedload Transport Measurements in a Steep Mountain Stream, Geophysical Research Letters, 46, 2019.

Meyer-Peter, E. and Müller, R.: Formulas for Bed-Load transport, IAHSR 2nd meeting, Stockholm, appendix 2, 1948.

Monsalve, A. and Yager, E. M.: Bed Surface Adjustments to Spatially Variable Flow in Low Relative Submergence Regimes: BED SURFACE ADJUSTMENTS IN LRS, Water Resources Research, 53, 2017.

Monteith, H. and Pender, G.: Flume investigations into the influence of shear stress history on a graded sediment bed, Water Resources Research, 41, https://doi.org/10.1029/2005WR004297, 2005.

Moog, D. B. and Whiting, P. J.: Annual hysteresis in bed load rating curves, Water Resour. Res., 34, 2393–2399, https://doi.org/10.1029/98WR01658, 1998.

Mueller, E. R., Pitlick, J., and Nelson, J. M.: Variation in the reference Shields stress for bed load transport in gravel-bed streams and rivers: VARIATION IN THE REFERENCE SHIELDS STRESS, Water Resour. Res., 41, https://doi.org/10.1029/2004WR003692, 2005.

Ockelford, A., Woodcock, S., and Haynes, H.: The impact of inter-flood duration on non-cohesive sediment bed stability, Earth Surface Processes and Landforms, 44, 2019.

Ockelford, A.-M. and Haynes, H.: The impact of stress history on bed structure, Earth Surface Processes and Landforms, 38, 717–727, https://doi.org/10.1002/esp.3348, 2013.

PAPHITIS, D. and Collins, M. B.: Sand grain threshold, in relation to bed "stress history": An experimental study, Sedimentology, 52, 827–838, https://doi.org/10.1111/j.1365-3091.2005.00710.x, 2005.

Parker, G.: On the cause and characteristic scales of meandering and braiding in rivers, J. Fluid Mech., 76, 457, https://doi.org/10.1017/S0022112076000748, 1976.

Parker, G.: Surface-based bedload transport relation for gravel rivers, Journal of Hydraulic Research, 28, 417–436, https://doi.org/10.1080/00221689009499058, 1990.

Phillips, C. B. and Jerolmack, D. J.: Self-organization of river channels as a critical filter on climate signals, Science, 352, 694–697, https://doi.org/10.1126/science.aad3348, 2016.

Phillips, C. B., Masteller, C. C., Slater, L. J., Dunne, K. B. J., Francalanci, S., Lanzoni, S., Merritts, D. J., Lajeunesse, E., and Jerolmack, D. J.: Threshold constraints on the size, shape and stability of alluvial rivers, Nat Rev Earth Environ, 1–14, https://doi.org/10.1038/s43017-022-00282-z, 2022.

https://doi.org/10.5194/egusphere-2024-3250
Preprint. Discussion started: 10 December 2024

Powell, D. M., Ockelford, A., Rice, S. P., Hillier, J. K., Nguyen, T., Reid, I., Tate, N. J., and Ackerley, D.: Structural properties of mobile armors formed at different flow strengths in gravel-bed rivers: Mobile Armor Structure, J. Geophys. Res. Earth Surf., 121, 1494–1515, https://doi.org/10.1002/2015JF003794, 2016.

Powell, M. and Ashworth, P.: Spatial Pattern of Flow Competence and Bed Load Transport in a Divided Gravel Bed River, Water Resources Research - WATER RESOUR RES, 31, 741–752, https://doi.org/10.1029/94WR02273, 1995.

Prancevic, J. P. and Lamb, M. P.: Particle friction angles in steep mountain channels, Journal of Geophysical Research: Earth Surface, 120, 242–259, https://doi.org/10.1002/2014JF003286, 2015.

Pretzlav, K. L. G., Johnson, J. P. L., and Bradley, D. N.: Smartrock Transport in a Mountain Stream: Bedload Hysteresis and Changing Thresholds of Motion, Water Resources Research, 56, e2020WR028150, https://doi.org/10.1029/2020WR028150, 2020.

Recking, A.: A comparison between flume and field bed load transport data and consequences for surface-based bed load transport prediction, Water Resources Research, 46, https://doi.org/10.1029/2009WR008007, 2010.

Reid, I., Frostick, L. E., and Layman, J. T.: The incidence and nature of bedload transport during flood flows in coarse-grained alluvial channels, Earth Surface Processes and Landforms, 10, 1985.

Rickenmann, D.: Variability of Bed Load Transport During Six Summers of Continuous Measurements in Two Austrian Mountain Streams (Fischbach and Ruetz), Water Resources Research, 54, 2018.

Rickenmann, D.: Effect of Sediment Supply on Cyclic Fluctuations of the Disequilibrium Ratio and Threshold Transport Discharge, Inferred From Bedload Transport Measurements Over 27 Years at the Swiss Erlenbach Stream, Water Resources Research, 56, e2020WR027741, https://doi.org/10.1029/2020WR027741, 2020.

Rickenmann, D. and McArdell, B. W.: Continuous measurement of sediment transport in the Erlenbach stream using piezoelectric bedload impact sensors, Earth Surface Processes and Landforms, 32, 1362–1378, https://doi.org/10.1002/esp.1478, 2007.

Rickenmann, D., Antoniazza, G., Nicollier, T., Wyss, C., Boss, S., Fritschi, B., Steeb, N., and Badoux, A.: Sediment transport observations in Swiss mountain streams, , http://dx.doi.org/10.16904/envidat.459, 2020.

Roberts, M. O., Renshaw, C. E., Magilligan, F. J., and Brian Dade, W.: Field Measurement of the Probability of Coarse-Grained Sediment Entrainment in Natural Rivers, Journal of Hydraulic Engineering, 146, 04020024, https://doi.org/10.1061/(ASCE)HY.1943-7900.0001694, 2020.

Roth, D. L., Finnegan, N. J., Brodsky, E. E., Rickenmann, D., Turowski, J. M., Badoux, A., and Gimbert, F.: Bed load transport and boundary roughness changes as competing causes of hysteresis in the relationship between river discharge and seismic amplitude recorded near a steep mountain stream, Journal of Geophysical Research: Earth Surface, 122, 2017.

Saletti, M., Molnar, P., Zimmermann, A., Hassan, M. A., and Church, M.: Temporal variability and memory in sediment transport in an experimental step-pool channel, Water Resources Research, 51, 2015.

Schuerch, P., Densmore, A. L., McArdell, B. W., and Molnar, P.: The influence of landsliding on sediment supply and channel change in a steep mountain catchment, Geomorphology, 78, 222–235, https://doi.org/10.1016/j.geomorph.2006.01.025, 2006.

https://doi.org/10.5194/egusphere-2024-3250
Preprint. Discussion started: 10 December 2024

Shields, A.: Application of similarity principles and turbulence research to bed-load movement, Retrieved January 13, 2021.

Shobe, C. M., Tucker, G. E., and Rossi, M. W.: Variable-Threshold Behavior in Rivers Arising From Hillslope-Derived Blocks, Journal of Geophysical Research: Earth Surface, 123, 1931.

Tucker, G. E. and Bras, R. L.: A stochastic approach to modeling the role of rainfall variability in drainage basin evolution, Water Resources Research, 36, 1953.

Turowski, J. M., Yager, E. M., Badoux, A., Rickenmann, D., and Molnar, P.: The impact of exceptional events on erosion, bedload transport and channel stability in a step-pool channel, Earth Surf. Process. Landforms, 34, 1661–1673, https://doi.org/10.1002/esp.1855, 2009.

Turowski, J. M., Badoux, A., and Rickenmann, D.: Start and end of bedload transport in gravel-bed streams, Geophysical Research Letters, 38, https://doi.org/10.1029/2010GL046558, 2011.

Turowski, J. M., Wyss, C. R., and Beer, A. R.: Grain size effects on energy delivery to the streambed and links to bedrock erosion, Geophysical Research Letters, 42, 1775–1780, https://doi.org/10.1002/2015GL063159, 2015.

Wiberg, P. L. and Smith, J. D.: Calculations of the critical shear stress for motion of uniform and heterogeneous sediments, Water Resour. Res., 23, 1471–1480, https://doi.org/10.1029/WR023i008p01471, 1987.

Wilcock, P. R. and Crowe, J. C.: Surface-based Transport Model for Mixed-Size Sediment, Journal of Hydraulic Engineering, 129, 120–128, https://doi.org/10.1061/(ASCE)0733-9429(2003)129:2(120), 2003.

Wong, M. and Parker, G.: Reanalysis and Correction of Bed-Load Relation of Meyer-Peter and Müller Using Their Own Database, Journal of Hydraulic Engineering, 132, 1159–1168, https://doi.org/10.1061/(ASCE)0733-9429(2006)132:11(1159), 2006.

Yager, E. M.: Prediction of sediment transport in steep, rough streams, (PhD thesis), 2006.

Yager, E. M., Turowski, J. M., Rickenmann, D., and McArdell, B. W.: Sediment supply, grain protrusion, and bedload transport in mountain streams, Geophysical Research Letters, 39, 2012.

Yager, E. M., Schmeeckle, M. W., and Badoux, A.: Resistance Is Not Futile: Grain Resistance Controls on Observed Critical Shields Stress Variations, Journal of Geophysical Research: Earth Surface, 123, 2018.